Sussex Research Online

Quantitative diagnostics of ancient paper using THz time-domain spectroscopy

Article (Accepted Version)

Missori, M, Pawcenis, D, Bagniuk, J, Mosca Conte, A, Violante, C, Maggio, M S, Peccianti, M, Pulci, O and Lojewskab, J (2018) Quantitative diagnostics of ancient paper using THz time-domain spectroscopy. Microchemical Journal, 142. pp. 54-61. ISSN 0026-265X

This version is available from Sussex Research Online: http://sro.sussex.ac.uk/id/eprint/76383/

This document is made available in accordance with publisher policies and may differ from the published version or from the version of record. If you wish to cite this item you are advised to consult the publisher's version. Please see the URL above for details on accessing the published version.

Copyright and reuse:
Sussex Research Online is a digital repository of the research output of the University.

Copyright and all moral rights to the version of the paper presented here belong to the individual author(s) and/or other copyright owners. To the extent reasonable and practicable, the material made available in SRO has been checked for eligibility before being made available.

Copies of full text items generally can be reproduced, displayed or performed and given to third parties in any format or medium for personal research or study, educational, or not-for-profit purposes without prior permission or charge, provided that the authors, title and full bibliographic details are credited, a hyperlink and/or URL is given for the original metadata page and the content is not changed in any way.

http://sro.sussex.ac.uk

Quantitative diagnostics of ancient paper using THz time-domain spectroscopy

M. Missori[a,*], D. Pawcenis[b], J. Bagniuk[b], A. Mosca Conte[c], C. Violante[c], M. S. Maggio[a], M. Peccianti[d], O. Pulci[c], J. Łojewska[b]

[a] *Istituto dei Sistemi Complessi, Consiglio Nazionale delle Ricerche, Unit Sapienza, Rome, Italy*
[b] *Faculty of Chemistry, Jagiellonian University, Ingardena 3, 30-060 Krakow, Poland*
[c] *ETSF, Dipartimento di Fisica, Universitá di Roma Tor Vergata, Rome, Italy*
[d] *Emergent Photonics Lab, Department of Physics and Astronomy, University of Sussex, Brighton, UK*

Abstract

In this work we have studied the terahertz spectra of modern artificially aged and ancient paper samples using terahertz time-domain spectroscopy. Hydrothermal artificial ageing was performed in closed and open reactors. Ancient paper samples were produced during the 15^{th} century in European countries. The main aim of the work is the quantitative assessment of spectral feature observed by terahertz spectroscopy as a function of degradation. To this goal, the state of degradation of paper samples was characterized by crystallinity measurements obtained by using X-ray diffraction and by the degree of polymerization of cellulose polymers obtained by size exclusion chromatography. The behavior of the terahertz spectra was formerly investigated as a function of the hydration of paper samples. This allowed discriminating between the spectral features induced by the presence of water and those induced by degradation of paper. Results indicate clear dependences of spectral parameters from the evolution of crystallinity and the degree of polymerization. They can be used as a nondestructive analytical method to assess the state of degradation of ancient paper by terahertz spectroscopy.

Keywords: Terahertz spectroscopy; Cellulose degradation; Paper ageing; X-ray diffraction of semicrystalline polymers; Molecular weight determination; Time-dependent density functional theory

1. Introduction

Cellulose-based materials have had several applications since the ancient times [1]. In particular, cellulose has played an important role in human civi-

*Corresponding author
Email addresses: mauro.missori@isc.cnr.it (M. Missori), olivia.pulci@roma2.infn.it (O. Pulci), lojewska@chemia.uj.edu.pl (J. Łojewska)

lization because it has been widely used for the production of paper and textile. Nowadays paper is used for applications spanning from packaging to electrical insulators in power transformers to production of biocompatible materials in medicine and pharmaceutical industry [2, 3]. However, since it was invented in China in the 1^{st} century A.D., its main application has been as writing support and medium for storing human knowledge. As a result a huge number of books, graphic works and ancient documents have been accumulating in archives, libraries and museums all over the world.

In Middle Ages and up to the middle 19^{th} century paper was obtained from pure cellulose fibers from linen, hemp or cotton raws, grinded in water with the addition of lime (calcium-containing inorganic mineral in which carbonates, oxides, and hydroxides predominate), and then drained through a sieve, pressed and dried, to obtain a sheet composed of a network of randomly interwoven fibers [4]. Animal glue was added as sizing compound. The resulting materials showed an excellent durability, and a large amount of ancient paper appears to be in a good conservation state.

Diagnostics methods able to provide information about the physical and chemical properties of ancient paper are however needed in order to quantitatively asses its state of conservation. Particularly important are nondestructive diagnostics methods, in particular spectroscopic methods using non-ionizing radiation allowing easy and safe access to the radiation beam for the artefact and avoiding a direct contact with its surface [5, 6]. This is particularly true for paper and cellulose artefact made of delicate organic matter.

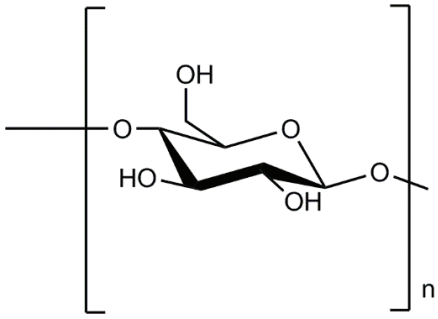

Figure 1: The monomer unit of the cellulose polymer.

The polymeric unit of cellulose is composed of β-D-glucopyranose units forming long polymeric chains of the order of thousands of monomers bonded by β-(l$\rightarrow$4)-glycosidic linkages. The equatorial conformation of β-linked glucopyranose residues (-OH) stabilizes the chair conformation structure of cellulose by the formation of both intermolecular and intramolecular hydrogen bonds.

The intermolecular hydrogen bonds are the predominant factor responsible for interchain cohesion. Overall, cellulose fibers have a pseudo-crystalline structure, composed of randomly distributed highly ordered (crystalline) domains and disordered (amorphous-like) regions [7]. The relative amount of polymer within the crystalline domains covers a wide range and depends on the origin and pretreatment of the sample, for native cotton cellulose being around 60-70% [8].

A system of pores and voids is contained within the paper structure. They are of nanometric size when fully confined in the amorphous regions, while they extend up to hundreds of nanometers within the cellulose fibres in paper. Pores within the paper structure are closely related to its density that is determined during papermaking. Pores and voids strongly influence the reactivity of cellulose due to water and external agent accessibility [9, 10].

Water molecules can be absorbed by cellulose wherever hydroxyl groups are available. The interaction between cellulose and water always occurs at the surface of crystalline domains or within amorphous regions. As a consequence the cellulose fibres, and paper as whole, absorb water into its structure. This phenomenon is called hydration. Under ambient conditions, at about 20°C temperature and 50% relative humidity (RH), paper contains from 5 to 8% of water in weight. Drying paper in a dry environment at room temperature reduces the number of water molecules up to about 2% [11]. A minimal amount of water makes part of the paper structure itself bridging different cellulose chains or it is H bonded to hydroxyl groups at the available surfaces: this is called bound water. Water that can be removed by drying is called free water [11, 9].

Paper ageing is initiated by external environmental factors, such as light, temperature, pollution and humidity, and by internal factors, such as pH, presence of impurities or additives (due to inks, sizing and fillers, by-products of degradation reactions) which may promote the hydrolysis β-D-glucopyranose units and the oxidation of β-(l→4)-glycosidic linkages [12, 13, 14].

These reactions are accompanied by the rearrangement of the H bond network and the consumption of the amorphous regions where both reactions proceed. As a consequence degradation causes an increase of the relative amount of polymer within the crystalline domains [8].

Terahertz (THz) science is a growing field of research thanks to an intense interaction between physics and engineering disciplines. This has made possible the development of systems to generate, detect and manipulate broadband coherent THz radiation [15]. THz spectroscopy is an active research field in chemistry, physics and biology, allowing detecting and identifying low-energy vibrational mode and excitation in molecules and condensed matter [16, 17]. In addition, it is exploited in industrial product diagnostics and in security applications [18].

Terahertz time-domain spectroscopy (THz-TDS) is a suitable approach to study low-energy vibrational properties of biological materials in a nondestructive way. The THz photon energy range (about 1-40 meV) is particularly suitable to probe the H bonds between molecules. THz-TDS is able to probe the

crystallinity of several materials, due to the interaction of THz radiation with optical phonons in crystal lattices[19].

For these reasons, THz-TDS was applied to the assessment of the state of degradation of single freely standing paper sheets providing clear fingerprints in the THz spectral profiles [20]. This was achieved by developing a new procedure to remove from the experimental signals the spurious interference effects generated by the Fabry-Pérot resonances in the sheets [21]. By using this approach, the THz absorption coefficient of cellulose fibers in ancient and modern samples artificially aged were obtained. A complex evolution of the spectra as a function of natural and artificial aging was found and qualitatively explained with a reduction of the H bond density in the cellulose polymer networks and an increasing of the sample crystallinity as consequence of hydrolytic and oxidative degradation of cellulose in paper.

In this paper, the THz spectra of modern artificially aged and ancient samples are studied in correlation with other quantitative diagnostic methods. For the appraisal of cellulose de-polymerisation, size exclusion chromatography (SEC) was used while samples crystallinity was estimated by using X-ray diffraction (XRD). The effect of the hydration of paper on THz spectra was studied by performing measurements with samples enclosed in a variable RH measurement chamber. In this way the contribution of free and bound water as well as that of bulk cellulose on the THz spectra was clearly identified and quantified. The residual absorption of bound water and the spectral background due to H bonds density was also correlated with cellulose de-polymerisation and crystallinity. The features of the peak at 2.15 THz due to the crystalline domains were also studied as a function of degradation.

2. Materials and methods

Samples. In this work, both modern as well as ancient samples were studied. Modern samples, named P2, were sourced from the Netherlands Organization for Applied Scientific Research (TNO). They are made of pure cotton linters cellulose, lignin free and ash content less than 0.005% in weight [13].

Ancient samples were produced during the 15^{th} century in European countries, consisting of 4 specimens, bearing no print, sized with gelatine as was customary in ancient times to improve the paper writing quality. They are labeled A1 and B1 (both made in Perpignan, France, in 1413) in good and in intermediate conservation conditions, respectively; A3 (made in Milan, Italy, in 1430) in bad conservation conditions due to the occurrence of a water spot in the past; and N1 made in Nuremberg (Germany), in the 15^{th} century, showing very bad state [22, 23, 24].

P2 samples were aged under two different conditions as reported in Table 1. Aging in P2C conditions was performed for 6, 12, 24 and 48 days, while in P2V conditions for 6, 12, 24 and 47 days. After the artificial aging the modern samples were named P2REF (unaged) and P2Cx and P2Vy where x = 06, 12, 24 and 48, and y = 06, 12, 24 and 47 [13].

Label	Aging reactor type	Aging conditions	Expected impact factors
P2C	Open (climatic chamber)	Air, RH=59%, T=90°C	Air and water vapor
P2V	Closed (vial)	Air, RH=59%, T=90°C	Air, water vapor and gaseous byproducts

Table 1: Environmental conditions used in the aging of P2 samples. RH indicates the relative humidity and T the temperature. Gaseous byproducts of cellulose degradation belong to various groups of organic compounds: aliphatic hydrocarbons, alcohols, aldehydes, ketones, carboxylic acids, esters, terpens and aromatic compounds [25]

.

Terahertz time-domain spectroscopy. The THz spectra were acquired in the transmission mode by using a Menlo Systems (Germany) TERA K15 THz time-domain spectrometer (THz-TDS). THz radiation was generated by photoconductive antennae allowing the optical to THz signal conversion. The antennae were excited by a femtosecond fiber-coupled laser (Menlo Systems T-Light) with center wavelength of 1560 nm, 100 MHz repetition frequency, and a pulse duration of nearly 90 fs [26]. The THz radiation emitted by the photoconductive antenna was collected and collimated in a beam with a diameter of about 20 mm by means of a TPX$^{\mathrm{TM}}$(polymethylpentene) lens with 50 mm nominal focal length. THz radiation was then focused onto the sample using another TPX$^{\mathrm{TM}}$lens with 100 mm nominal focal length. The samples were placed at the THz focus where the illuminated area was approximately 6 mm in diameter, so that the THz pulse could probe a large area, thus minimizing heterogeneity effects. The THz radiation transmitted through the sample was collected and collimated and then focused onto the detector antenna by another couple of 100 mm and 50 mm nominal focal length TPX$^{\mathrm{TM}}$lenses. Acquisitions were performed by averaging the THz pulses over 1600 scans of the delay line (each lasting 0.125 s), therefore the time for a single acquisition was 200 s (Fig. 2). The delay line scan range was 100 ps. Data were collected with a sampling step of 33.36 fs. Terahertz pulse data arrays were converted in spectral data by a standard FFT (Fast Fourier Transform) algorithm. Fabry-Perot interference effects were removed from spectral data by a numerical procedure able to extract the optical parameters from THz TDS spectral data of very thin samples [20, 21]. In this way the absorption coefficient of samples α_{paper} was obtained.

The paper samples consist of a random assembly of cellulose fibers and voids, in a sample dependent relative concentration. Typical sizes of fibers and voids are around 10-20 μm, i.e. much smaller than the wavelengths associated to the 0.2 –3.5 THz range (i.e., from 1500 μm to 86 μm). Therefore, THz radiation probes the volume averaged properties of the papers sheets. To recover the absolute absorption coefficient of cellulose fibers at THz frequencies, it is necessary to estimate the relative amount of cellulose in the paper sheets. This information can be recovered from the paper sample density (ρ_{paper}) which was

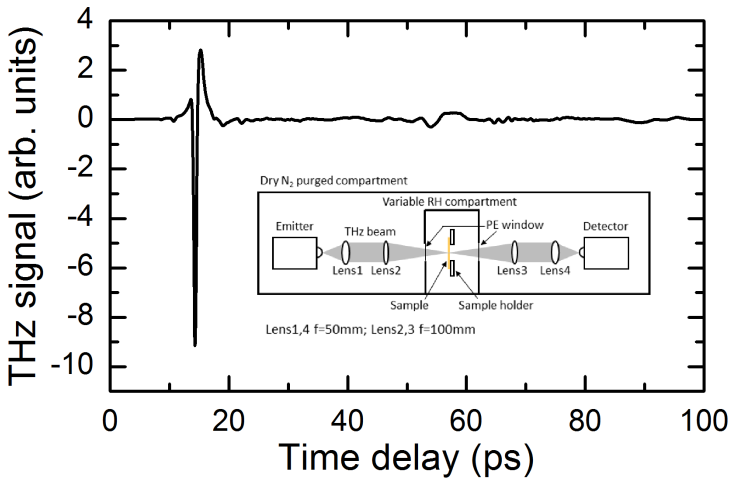

Figure 2: THz signals measured with P2REF sample at RH=2.7%. In the inset a sketch of the experimental set-up is also shown (PE indicates polyethylene).

measured according to the procedure described in Ref. [20]. The relative error in the values of ρ_{paper} is about 10%, essentially due to the uncertainty in the measurement of the sample thicknesses and weight, the last due to the unknown moisture content. The volume fraction v of cellulose fibers in the sample can be obtained by assuming $v = V_c/V_{paper} = \rho_{paper}/\rho_c$, where V_c and V_{paper} are the volume occupied by cellulose fibers and the volume of the paper sheets used in this study, respectively, while $\rho_c = 1.5\ g/cm^3$ is the average density of cellulose fibers. The values of v for the samples studied are reported in Table 2. Such numbers are required to calculate the absolute absorption coefficient (α) of cellulose fibers, given that THz radiation probes the volume averaged properties of the papers sheets [27, 24, 28, 20]:

$$\alpha = \frac{\alpha_{paper}}{v} \tag{1}$$

Since the water vapor absorbs THz radiation, the compartment of the spectrometer containing the photoconductive antennae and the lenses was purged with dry N_2 for 120 min before spectra acquisition until the water vapor absorption lines became indistinguishable from noise. In order to study the THz spectra of samples as a function of RH the sample holder was placed in separate compartment purged with variable humidity N_2 realized by flowing the N_2 through de-ionized water. Two thin polyethylene (PE) foils (thickness 80 μm) were used as windows for THz radiation transmission (Fig. 2). RH measurement were performed by using a Rotronic electronic thermo-hygrometer. All measurements were carried out at a temperature of (23 ± 1)°C.

Samples	$t(\mu m)$	$\rho_{paper}(g/cm^3)$	v
P2	90	0.84	0.56
A1	108	0.76	0.51
B1	102	0.71	0.47
A3	75	0.71	0.47
N1	124	0.91	0.61

Table 2: Mean thickness (t), densities (ρ_{paper}) and volume fractions (v) of the modern and ancient specimens measured in the experiments. The samples belonging to the P2C and P2V series (aged and not aged) show the same thickness within the experimental errors. The relative error of v is about 10% (see text for details).

X-ray diffraction. XRD measurements were performed on a Philips X'Pert Pro MPD diffractometer, using Cu Kα_1 line ($\lambda = 1.5405$ Å), equipped with a Johansson monochromator and silicon position sensitive X'Celerator detector. Diffractograms were measured in the 10-40 2θ range with 0.008 degree step and collection time of 240 seconds per step. During measurements, variable divergence slit was used allowing to obtain constant sensitivity through the whole range of 2θ.

XRD results were used to calculate crystallinity indexes (CI) using two methods: peak height method (CI_h) and deconvolution method (CI_d) both described in [29]. In peak height method CI_h is calculated from the ratio between the height of the 002 peak (I_{002}) and the height at the minimum at ca. $2\Theta = 19°$ (I_{AM}) related to the amorphous phase. In deconvolution method 5 peaks are fitted to simulate measured diffractogram: 4 of them refer to crystallite peaks and one is amorphous. The ratio between their areas is used to calculate CI_d [29] (Fig. 3). Due to the similarity of the results only CI_d will be used for correlation with THz spectra.

Degree of polymerization. Molar mass distribution measurements were carried out by using size exclusion chromatography (SEC) with multiple angle laser light scattering (MALLS) and differential refractometry index (DRI) detectors [13, 30]. Molar mass distributions of paper samples (derivatised to cellulose tricarbanilates) were determined with use of Waters chromatographic system which consists of isocratic pump 1515, autosampler 717+,column oven, MALLS detector (Dawn Heleos, Wyatt Technology, working at 658 nm) and differential refractive index detector (Opti-lab T-rEX, Wyatt Technology, working at 658 nm, maintained at 35°C) acting as a concentration sensitive detector. Separation of the cellulose tricarbanilate samples was performed with use of a set of two 25 cm × 1 cm mixed-bed polydivinylbenzene columns (Jordi). They were thermostated at 35°C and preceded by a guard column (Waters). Tetrahydrofuran (HPLC grade, J. T. Baker) was used as eluent with a flow rate of 1.0 cm^3/min. From SEC measurements different average molar masses are derived: number average molecular weight M_n, weight average molecular weight M_w and z-average molecular weight M_z. The DP is defined as the number of monomeric units in a polymer. For a homopolymer like cellulose the number-

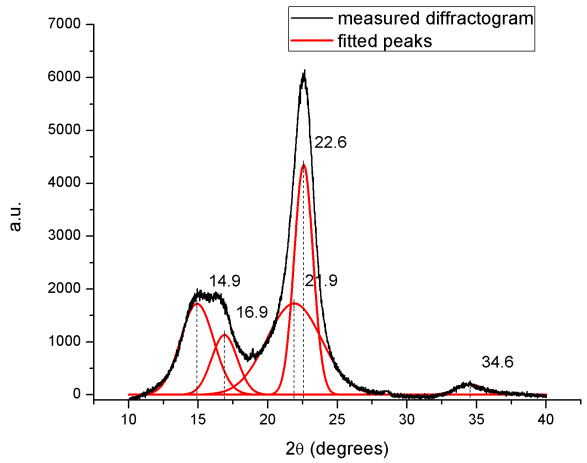

Figure 3: XRD results for P2REF sample. The 5 peaks used in the deconvolution method are represented: those at 14.9, 16.9 22.6 and 34.6° refer to crystallite peaks while that at 21.9° to the amorphous phase [29].

average degree of polymerization is given by DP = M_n/M_0, where M_0 is the molecular weight of the monomer unit. Hydrolysis of cellulose polymers is the principal cause of DP reduction. A typical trend in cellulose degradation is that in the initial stage the rate of DP decreasing is higher than in the advanced ageing; this is the cause of the so-called level-off degree of polymerization (LODP) [13, 31, 32].

DFT theoretical simulations. Cellulose was modeled as a crystal in its most common crystalline form (I_β phase), as in Refs. [24, 27, 28]. Both the unit cell and the atomic coordinates of the structures were relaxed by using a density-functional-theory plane-wave code with ultrasoft pseudopotentials (QUANTUM ESPRESSO [33]). For the unaged cellulose theoretical unit cell, the following Bravais vectors (expressed in Bohr) (19.31, -0.1494, 0.6432), (-0.1353, 15.19, -0.3923), and (0.1847, 8.144, 8.051) were obtained. In order to include Van der Waals (VdW) interactions in the total energy calculation, a VdW-DF2 [34] nonlocal density functional has been employed. This functional is an enhanced version of VdW-DF [35] and it is based on a more accurate semilocal exchange functional, the PW86 [36]. It was chosen to achieve a better description of the H-bonds [37]. A cutoff of 40 Ry for the Kohn-Sham wavefunctions and of 800 Ry for the charge density was employed. Proper ultrasoft pseudopotentials [38], conveniently generated [39] to be suitable for the nonlocal VdW functionals, were used. The Irreducible Brillouin Zone has been sampled with 14 k-points [24, 27, 28]. Vibrational properties have been calculated using finite displacements within the DFT framework, as described in Ref. [40]. We applied this

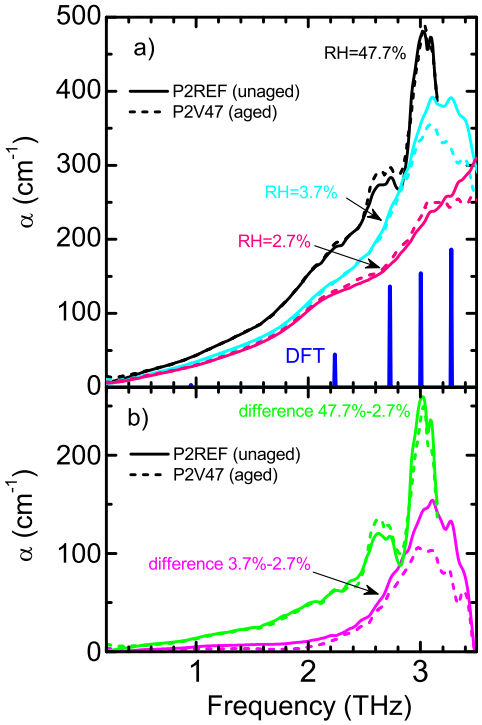

Figure 4: Panel a): absorption coefficients vs frequency of cellulose fibers in the unaged modern samples P2REF (solid lines) and in the artificially aged sample P2V47 (dashed lines) as a function of RH. Spectra acquired at RH=47.7% are shown up to 3.15 THz. The theoretical absorption frequencies for I_β phase cellulose obtained by DFT simulations are also shown. Panel b): differences of spectra acquired at RH=47.7% and RH=3.7% with respect to those acquired at RH=2.7% for sample P2REF (solid lines) and P2V47 (dashed lines).

approach for the calculation of the phononic eigenvalues and eigenfunctions at the Γ-point, to determine the cellulose THz absorption spectrum in its pristine form.

3. Results and discussion

The terahertz experimental absorption spectra of cellulose fibers in modern paper samples P2REF and P2V47 at 3 different values of RH is shown in Fig. 4. Overall, the absorption increases as a function of frequency showing, firstly, a monotonic increase from 0.2 THz to about 1.6 THz whose amplitude depends on RH. Superimposed to this trend, several different spectroscopic features, strongly dependent on RH, appear between 1.8 THz up to the upper limit of the spectra. A clear spectroscopic feature (shoulder) is always observed at about 2.15 THz. Samples measured at RH=47.7% also show well defined bands at

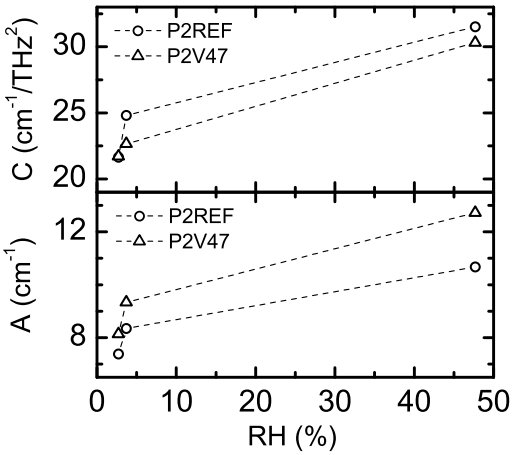

Figure 5: Values of coefficient A and C as function of RH for P2REF and P2V47 samples. Dashed lines are a guide for the eye.

about 2.6 and 3 THz. Samples measured at RH=3.7% show, instead, a strong reduction of the intensity of the band at 2.6 THz while the band at 3.0 THz appears to be reduced in intensity, broadened and shifted at about 3.1 THz. Finally, in samples measured at RH=2.7%, while the shoulder at 2.15 THz still appears well defined, only low intensity spectroscopic features are observed at higher frequencies. In particular, a small peak is observed at 3.1 THz for the P2V47 sample.

The interpretation of the terahertz spectra as a function of RH can be founded on the knowledge of the molecular and supramolecular structure of cellulose fiber in paper samples. Indeed, cellulose polymers in elementary fibers assembly through H bonds in crystalline and disordered (amorphous) regions. Indeed, the monotonic increase of the absorption is typically observed in the THz spectra of amorphous solids by H-bond networks [20, 41]. At the THz spectral regions these absorption spectra can be approximated by:

$$\alpha \simeq A + C\omega^{\beta} \tag{2}$$

where C is a numerical coefficient which is expected to be proportional to the density of H bonds, β is an exponent which is approximately 2 in glassy materials and A is a constant [42]. In a previous work, the non-vanishing values of the constant A were interpreted as due to the existence of residual water in the paper structure [20]. In all samples, regardless of RH, the absorption coefficient curve from 0.2 to 1.6 THz can be well approximated by Eq.2 function. However, the values of A and C coefficients obtained from a best-fit procedure appear to be dependent on RH. They are shown as a function of RH in Fig.

5. Values of both parameters decrease at smaller RH for both samples. These results can be explained by remembering that the moisture content of cellulosic materials decreases when RH decreases. Indeed, the decreasing amount of water embedded within the structure of paper decreases the H-bond density which is probed by the C coefficient. Also, the decreasing of A coefficient shown in Fig. 5 confirms the hypothesis that it is connected to the absorption of water present in the samples. The non-vanishing values of A and C for the lowest value of RH indicate that a small amount of water is still present within the structure of cellulose. In fact, a minimal amount of water is part of the paper structure itself bridging different cellulose chains. This also happens in other biological samples such as proteins, where there is always some amount of water (internal or bound water) that constitutes a structural part of the system and cannot be removed at room temperature [11, 9].

When RH is decreased from 47.7 to 2.7% C decreases of 9.9 and 8.6 $\mathrm{cm}^{-1}/\mathrm{THz}^2$ for P2REF and P2V47 respectively, and A decreases of 3.3 and 4.7 cm^{-1} for P2REF and P2V47 respectively. Therefore, the unaged sample P2REF shows higher reduction of the density of H bonds and a lower reduction of water content. The contrary happens for the aged sample P2V47 which shows a lower decreasing of H bond density and higher decreasing of water content. This behavior can be explained by the fact that the consequence of paper degradation is the rupture of H bonds linking cellulose polymers mostly within amorphous regions, thus enhancing the fibres accessible volume and the possibility for aged paper to retain higher amounts of free water. However, in the aged sample the newly accessible regions lost their hydrophilic character due to the progressive transformation of hydroxyl groups of glucopyranose units into carbonylic groups. This prevents the formation of cellulose-water H bond and, therefore, the presence of bound water [9].

The non vanishing values of A and C coefficients at the lowest RH as shown in Fig. 5 also suggest that their values do not depend only on the content of free or bound water in paper. Indeed, their higher values with respect to the extent of the changes induced by the RH variation suggest a not negligible contribution of cellulose. This can be expressed as:

$$\begin{aligned} A &= A_{cell} + A_{water} + A_{bw} \\ C &= C_{cell} + C_{water} + C_{bw} \end{aligned} \tag{3}$$

where A_{cell} and C_{cell} represent the contribution of cellulose, A_{water} and C_{water} that of free water in paper structure and A_{bw} and C_{bw} that of bound water at the cellulose fibers available sites. At ambient conditions, all three contributions concur to the measured values of A and C coefficients. When the RH is decreased in such a way that the contribution of free water is negligible (in our case at RH=2.7%) A represents the residual absorption of bulk cellulose and of water bound to cellulose while C represents the overall density of cellulose H bonds and water-cellulose hydrogen-bonded structures (bound water).

Since cellulose is made of amorphous and crystalline regions, the peaks due to

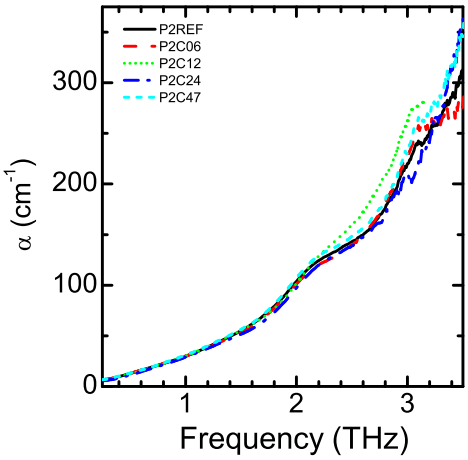

Figure 6: Absorption coefficients vs frequency of cellulose fibers in the modern samples artificially aged in P2C conditions (due to noise the spectrum of sample P2C12 has been truncated at 3.15 THz).

the crystalline phase should be superimposed to the disordered H-bond spectral background. However, as shown in Fig. 4, it is evident that hydration of paper strongly influences the terahertz regions where the crystalline phase peaks are expected to appear. Indeed, the spectra of P2REF and P2V47 samples acquired at RH 47.7% strongly differ from those acquired at RH=3.7 and 2.7% in the 2-3.5 THz spectral region. In panel b) of Fig. 4 this effect is evidenced by the differences of spectra with respect to those acquired at RH=2.7%. Beside the strong reduction in the bands amplitude, decreasing of RH also results in a shift towards higher frequencies. This effect has been also observed in other hydrated materials [43, 44].

In addition, since crystalline regions are believed to be not accessible to water molecules, the strong bands observed for the higher values of RH should be related to vibration of semi-crystalline domains. Indeed, less-ordered interlinking regions between the crystallites inside the elementary fibrils are expected according to the fringe-fibrillar model of fiber structure [8].

DFT simulations indicate that the THz spectral profile is composed of several peaks associated with long-range cellulose crystal phononic modes. The calculated peaks at about 2.2, 2.7, 3.0, and 3.3 THz appear to be in good agreement with the experimental ones obtained at higher values of RH. However, when RH is reduced the experiments show only two evident features at 2.15 and 3.1 THz. Since the paper hydration has a huge effect on the peaks of the crystalline phase this make difficult a suitable approach for cultural heritage characterization by THz TDS. Quantitative results correlating the intensity of THz peak at 2.15 and 3.1 THz and the CI obtained by XRD were obtained on

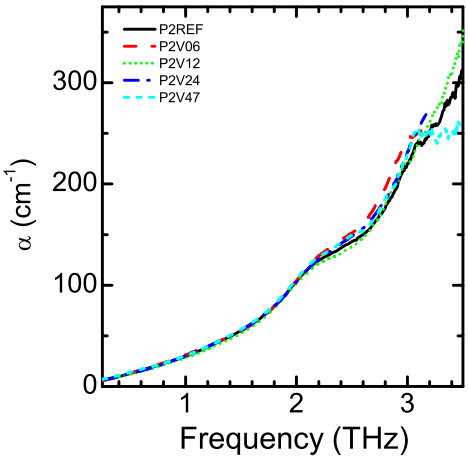

Figure 7: Absorption coefficients vs frequency of cellulose fibers in the modern samples artificially aged in P2V conditions (due to noise the spectra of samples P2V06 and P2V24 have been truncated at 3.15 THz).

microcrystalline cellulose submitted to ball milling procedures and equilibrated under dry N_2 for THz measurements [19].

Due to the strong influence of paper hydration on the THz spectra measurements on modern and ancient samples were performed at the lowest RH value (about $(2.7 \pm 0.3)\%$) obtainable by purging dry N_2 for at least 2 hours in the measurement compartments. The terahertz experimental absorption spectra of modern paper samples aged in P2C and P2V conditions are shown in Figures 6 and 7 respectively; those of ancient paper samples in Fig. 8. All modern and ancient paper spectra show the monotonic increase of absorption as a function of frequency from 0.2 to about 1.6 THz and, superimposed to this trend, a clear shoulder at about 2.15 THz. In addition, some samples show a peak at about 3.1 THz: this is particularly evident in sample N1 and less apparent in the most degraded samples of P2C and P2V series. The unaged or less degraded modern samples of P2C and P2V series show, instead, tiny spectroscopic features at 3.1 THz hardly distinguishable from noise.

Therefore, we concentrate on the study of the spectral features of the shoulder at about 2.15 THz. In order to separate the crystalline contribution from the disordered background, a subtraction of the Eq.2 term was performed for every sample, extending the background fit deduced from the initial behavior (0.2-1.6 THz) up to about 3 THz. A Gaussian fit of the resulting curve was performed from 1.55 to 2.3 THz. The best fit values of the peak position, width and intensity are shown in Fig. 9. Values appear to be scattered without showing clear trends. Within the investigated CI_d range the average peak positions is (2.16±0.03) THz and the average width is (0.22±0.02) THz. Values for peak

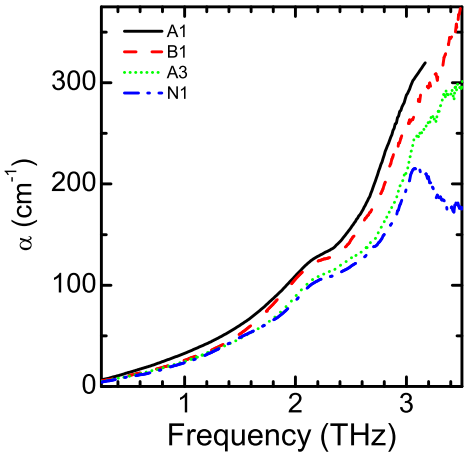

Figure 8: Absorption coefficients vs frequency of cellulose fibers in the ancient paper samples (due to noise the spectrum of samples A1 has been truncated at 3.17 THz).

intensity show the largest variance as a function of CI_d, however, even in this case, no clear trends emerge in the investigated CI_d range.

The lack of a clear trend in the 2.15 THz peaks parameters, already observed in a previous work [19], indicate that the aging and degradation of paper is a complex process in which chemical and structural phenomena compete. Since degradation primarily happens in the amorphous regions surrounding the crystalline domains [7, 8, 9], the peak parameters could be influenced by vibrational modes in the neighboring amorphous regions and also to the progressive degradation of the external surfaces of the crystalline domains, with consequent enhancements of finite-size effects in the phononic modes [45].

The behavior of A and C coefficients (Eq. 2) as a function of CI_d is shown in Fig. 11. Although values are scattered, in particular for ancient samples, evident trends emerge as a function of the increasing CI_d also in this case. Overall data indicate that A and C coefficients decrease with increasing CI_d. In fact, the increasing degradation of paper indicated by the crystallinity has as consequence the consumption of the amorphous regions with a consequent decreasing of the density of H bonds (C). The increasing oxidation of samples [13, 24] causes the lost of the hydrophilic character of the accessible regions due to the progressive transformation of hydroxyl groups into carbonylic groups (A).

The behavior of A and C coefficients as a function of DP is shown in Fig. 11. Although values are scattered, evident trends emerge as a function of the increasing DP also in this case. Overall data for ancient samples (open circles) indicate that A and C coefficients decrease with increasing DP. This is not true for the modern samples artificially aged which show an almost constant behavior of A and C coefficients as a function of DP (squares and triangles). These

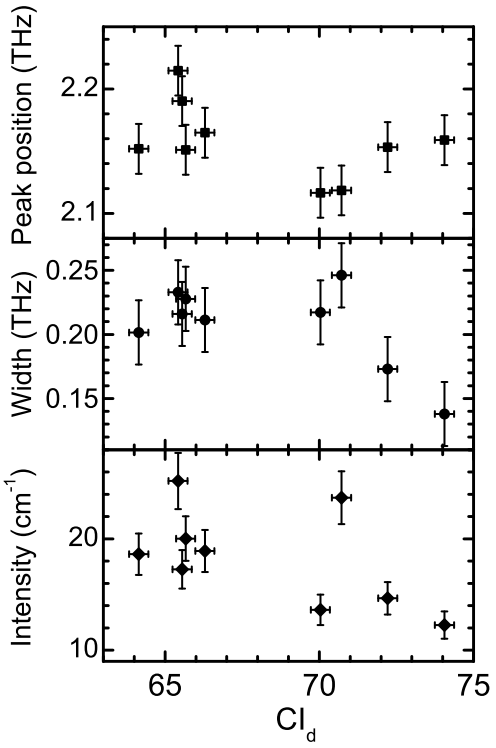

Figure 9: Peak position, width and intensity of the shoulder at about 2.15 THz as function of the cristallinity index CI_d of the P2V and ancient samples.

results are in agreement with those of Fig. 10 indicating that the performed artificial aging, even though it produces relevant chemical changes, it is not able to mimic the transformation of the supermolecular structure of cellulose fibers which happens in natural degradation.

4. Conclusions

In this work we have investigated the THz spectra of modern artificially aged and ancient paper samples using THZ TDS. The effect of paper hydration was preliminarily studied in order to clarify the origin of the observed spectral features. THz spectra of paper samples are composed of a Eq.2 background due to the contributions of disordered H-bond networks of cellulose, free and bound water. Spectral bands induced by cellulose polymers crystalline domains are superimposed to this background. In fact, THz-TDS is sensitive to the crystallinity of several materials due to the interaction of THz radiation with optical phonons in crystal lattices. DFT simulations confirm that the spectral profile is composed of several peaks associated with long-range cellulose crystal

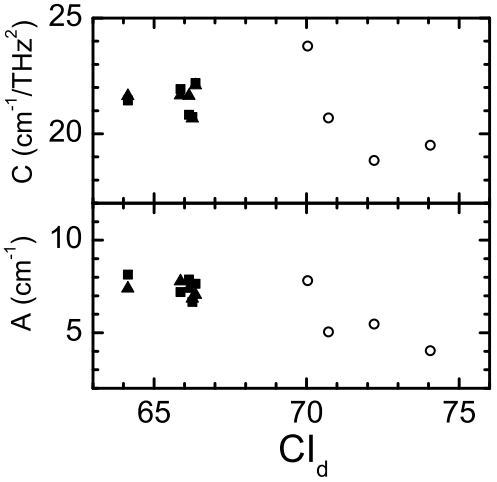

Figure 10: Values of coefficients A and C as a function of CI_d for ancient (open circles) and modern paper samples P2C (squares) and P2V (triangles). CI_d of P2C and P2V samples ranges from 64 to 67, that of ancient from 70 to 74.

phononic modes. The calculated peaks at about 2.2, 2.7, 3.0, and 3.3 THz appear to be in qualitative agreement with the experimental ones for higher values of RH. All these features are strongly dependent on the hydration of paper samples. Therefore, in order to limit the hydration effects, THz TDS measurements were performed at the lowest available RH value. In such a way it was possible to correlate the behaviour of A and C coefficient and the intensity, width and peak position of the band at 2.15 THz with the crystallinity index CI_d obtained by XRD and with DP obtained by SEC. Results show the capability of THz TDS to detect chemical and physical changes of cellulose fibers in paper artefacts. This approach could be used as a nondestructive analytical method to estimate the state of degradation of ancient paper.

5. Acknowledgements

M. M. acknowledges funding from the Ministero dell'Istruzione, dell'Università e della Ricerca under Progetto Premiale THEIA. M. M., M. S. M. and M. P. acknowledge funding from the Regione Lazio under Progetto Torno Subito 2015. M. P. acknowledges funding from European Unions Seventh Framework Programme for research, technological development and demonstration under grant agreement no 630833 and from the European Unions Horizon 2020 research and innovation Programme, grant agreement no 725046. We acknowledge CINECA for cpu hours provided by projects: IsB05_LEONAR_E, IsB03_PAPER, IsB05_LEONARDO. The research was carried out with the equipment (Opitilab t-rEX detector, Wyatt Technology) purchased thanks to the financial support of

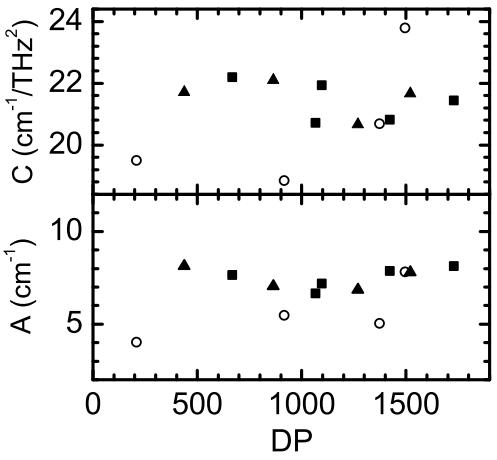

Figure 11: Values of coefficients A and C as a function of DP for ancient (open circles) and modern paper samples P2C (squares) and P2V (triangles).

the European Regional Development Fund in the framework of the Polish Innovation Economy Operational Program (contract no. POIG.02.01.00-12-023/08).

References

[1] D. Hunter, Papermaking: The History and Technique of an Ancient Craft, Dover Pubns, New York, 1978.

[2] D. Klemm, B. Heublein, H. P. Fink, A. Bohn, Cellulose: fascinating biopolymer and sustainable raw material, Angew. Chem. Int. Ed. 44 (2005) 3358–3393. doi:doi:10.1002/anie.200460587.

[3] S. Schabel, H.-J. Schaffrath (Eds.), Progress in Paper Physics Seminar, Darmstadt (Germany), 2016.
URL www.tuprints.ulb.tu-darmstadt.de/5636

[4] J. Dabrowski, J. S. G. Simmons, Permanance of early european hand-made papers, Fibres Text. East. Eur. 11 (1) (2003) 8–13.

[5] K. K. Janssens, R. Van Grieken (Eds.), Non-Destructive Microanalysis of Cultural Heritage Materials, Vol. XLII of Comprehensive Analytical Chemistry, Elsevier, 2004.

[6] K. Fukunaga, THz Technology Applied to Cultural Heritage in Practice, Springer, 2016. doi:10.1007/978-4-431-55885-9.

[7] D. Klemm, B. Philipp, T. Heinze, U. Heinze, W. Wagenknecht, Comprehensive Cellulose Chemistry Volume I, WILEY-VCH Verlag GmbH, Weinheim, 1998.

[8] H. A. Krassig, Cellulose: Structure, Accessibility, and Reactivity, Gordon and Breach Science Publishers, Singapore, 1993.

[9] C. Corsaro, D. Mallamace, S. Vasi, L. Pietronero, F. Mallamace, M. Missori, The role of water in the degradation process of paper using 1h hr-mas nmr spectroscopy, Phys. Chem. Chem. Phys. 18 (2016) 33335–33343. doi:10.1039/c6cp06601a.

[10] D. Mallamace, S. Vasi, M. Missori, C. Corsaro, New insight into hydration and aging mechanisms of paper by the line shape analysis of proton nmr spectra, Il Nuovo Cimento C 39 (2016) 309–319. doi:10.1007/s11467-017-0686-6.

[11] I. Brueckle, Structure and properties of dry and wet paper, in: G. Banik, I. Brueckle (Eds.), Paper and Water: A guide for conservators, Routledge, London and New York, 2011, Ch. 4, pp. 81–119.

[12] S. Zervos, Natural and accelerated ageing of cellulose and paper: A literature review, in: A. Lejeune, T. Deprez (Eds.), Cellulose: Structure and Properties, Derivatives and Industrial Uses, Nova Publishing, New York, 2010, Ch. 5, pp. 155–203.

[13] T. Łojewski, K. Zieba, A. Knapik, J. Bagniuk, A. Lubańska, J. Łojewska, Evaluating paper degradation progress. cross-linking between chromatographic, spectroscopic and chemical results, Appl. Phys. A 100 (2010) 809–821. doi:10.1007/s00339-010-5657-5.

[14] P. Łojewski, P. Miśkowiec, M. Missori, A. Lubańska, L. Proniewicz, J. Łojewska, Ftir and uv/vis as methods for evaluation of oxidative degradation of model paper: Dft approach for carbonyl vibrations, Carbohydr. Polym. 82 (2010) 370. doi:10.1016/j.carbpol.2010.04.087.

[15] Y. Lee, Principles of Terahertz Science and Technology, Springer Science+Business Media, LLC, 2009.

[16] Y. Ueno, K. Ajito, Analytical terahertz spectroscopy, Anal Sci 24 (2008) 185–192. doi:10.2116/analsci.24.185.

[17] J.-H. Son, Terahertz Biomedical Science & Tecnology, CRC Press, 2014.

[18] P. U. Jepsen, D. G. Cooke, M. Koch, Terahertz spectroscopy and imaging - modern techniques and applications, Laser Photonics Rev. 5 (1) (2011) 124–166. doi:10.1002/lpor.201200505.

[19] F. S. Vieira, C. Pasquini, Determination of cellulose crystallinity by terahertz-time domain spectroscopy, Anal. Chem. 86 (2014) 3780–3786. doi:10.1021/ac4035746.

[20] M. Peccianti, R. Fastampa, A. Mosca Conte, O. Pulci, C. Violante, J. Łojewska, M. Clerici, R. Morandotti, M. Missori, Terahertz absorption by cellulose: Application to ancient paper artifacts, Phys. Rev. Appl 7 (2017) 064019. doi:10.1103/physrevapplied.7.064019.

[21] R. Fastampa, L. Pilozzi, M. M, Cancellation of fabry-perot interference effects in terahertz time-domain spectroscopy of optically thin samples, Phys Rev A 95 (2017) 063831. doi:10.1103/physreva.95.063831.

[22] M. Missori, M. Righini, S. Selci, Optical reflectance spectroscopy of ancient papers with discoloration or foxing, Opt. Commun. 231 (2004) 99–106. doi:10.1016/j.optcom.2003.12.034.

[23] A. Mosca Conte, O. Pulci, A. Knapik, J. Bagniuk, R. Del Sole, J. Łojewska, M. Missori, Role of cellulose oxidation in the yellowing of ancient paper, Phys. Rev. Lett. 108 (2012) 158301. doi:10.1103/physrevlett.108.158301.

[24] A. F. Mosca Conte, O. Pulci, M. Misiti, J. Łojewska, L. Teodonio, C. Violante, M. Missori, Visual degradation in leonardo da vinci's iconic self-portrait: a nanoscale study, Appl. Phys. Lett. 104 (2014) 224101. doi:10.1063/1.4879838.

[25] T. Łojewski, K. Ziebla, A. Knapik, J. Bagniuk, A. Lubańska, J. Łojewska, Furfural as a marker of cellulose degradation. a quantitative approach, Appl. Phys. A 100 (2010) 809–821. doi:10.1007/s00339-010-5663-7.

[26] A. Ferraro, D. C. Zografopoulos, M. Missori, M. Peccianti, R. Caputo, R. Beccherelli, Flexible terahertz wire grid polarizer with high extinction ratio and low loss, Opt. Lett. 41 (2016) 2009–2012. doi:10.1364/ol.41.002009.

[27] M. Missori, O. Pulci, L. Teodonio, C. Violante, I. Kupchak, J. Bagniuk, J. Łojewska, A. Mosca Conte, Optical response of strongly absorbing inhomogeneous materials: application to paper degradation, Phys. Rev. B 89 (2014) 054201. doi:10.1103/physrevb.89.054201.

[28] C. Violante, L. Teodonio, A. Mosca Conte, O. Pulci, I. Kupchak, M. Missori, An ab-initio approach to cultural heritage: The case of ancient paper degradation, Physica Status Solidi B 252 (2015) 112–117. doi:10.1002/pssb.201350403.

[29] S. Park, J. O. Baker, M. E. Himmel, P. P. A, J. D. K, Celullose crystallinity index: measurement techniques and their impact on interpreting cellulase performance, Biotechnology for Biofuels 3 (2010) 10. doi:10.1186/1754-6834-3-10.

[30] L. Teodonio, M. Missori, D. Pawcenis, J. Łojewska, F. Valle, Nanoscale analysis of degradation processes of cellulose fibers, Micron 91 (2016) 75. doi:10.1016/j.micron.2016.07.013.

[31] J. Daňhelka, I. Kössler, V. Boháčková, Determination of molecular weight distribution of cellulose by conversion into tricarbanilate and fractionation, J Polym Sci 14 (1976) 287298. doi:10.1002/pol.1976.170140202.

[32] T. Lojewski, K. Zieba, J. Lojewska, Size exclusion chromatography andviscometry in paper degradation studies: New mark-houwink coefficients forcellulose in cupri-ethylenediamine, Journal of Chromatography A 1217 (2010) 64626468. doi:10.1002/mrc.4127.

[33] P. Giannozzi, S. Baroni, N. Bonini, M. Calandra, R. Car, C. Cavazzoni, D. Ceresoli, G. Chiarotti, M. Cococcioni, I. Dabo, A. Dal Corso, S. de Gironcoli, S. Fabris, G. Fratesi, R. Gebauer, U. Gerstmann, C. Gougoussis, A. Kokalj, M. Lazzeri, L. Martin-Samos, N. Marzari, F. Mauri, R. Mazzarello, S. Paolini, A. Pasquarello, L. Paulatto, C. Sbraccia, S. Scandolo, G. Sclauzero, P. Ari Seitsonen, A. Smogunov, P. Umari, R. M. Wentzcovitch, Quantum espresso: a modular and open-source software project for quantum simulations of materials, Journal of Physics: Condensed Matter 21 (39) (2009) 395502. doi:10.1088/0953-8984/21/39/395502.

[34] K. Lee, E. D. Murray, L. Kong, B. I. Lundqvist, D. C. Langreth, Higher-accuracy van der waals density functional, Phys. Rev. B 82 (2010) 081101(R). doi:10.1103/physrevb.82.081101.

[35] M. Dion, H. Rydberg, E. Schroder, D. Langreth, I. B. Lundqvist, Van der waals density functional for general geometries, Phys. Rev. Lett. 92 (2004) 246401.

[36] J. Perdew, Y. Wang, Accurate and simple density functional for the electronic exchange energy: Generalized gradient approximation, Phys. Rev. B 33 (1986) 8800(R). doi:10.1103/physrevb.40.3399.

[37] A. K. Kelkkanen, B. I. Lundqvist, J. K. Norskov, Density functional for van der waals forces accounts for hydrogen bond in benchmark set of water hexamers, Chem. Phys. 131 (2009) 046102. doi:10.1063/1.3193462.

[38] D. Vanderbilt, Soft self-consistent pseudopotentials in a generalized eigenvalue formalism, Phys. Rev. B 41 (1990) 7892(R). doi:10.1103/physrevb.41.7892.

[39] R. Sabatini, T. Gorni, S. de Gironcoli, Nonlocal van der waals density functional made simple and efficient, Phys. Rev. B 87 (2013) 041108(R). doi:10.1103/physrevb.87.041108.

[40] A. Calzolari, M. Buongiorno Nardelli, Dielectric properties and raman spectra of zno from a first principles finite-differences/finite-fields approach, Sci. Rep. 3 (2013) 2999. doi:10.1038/srep02999.

[41] E. Scarpellini, M. Ortolani, A. Nucara, L. Baldassarre, M. Missori, R. Fastampa, R. Caminiti, Stabilization of the tensile strength of aged cellulose paper by cholinium-amino acid ionic liquid treatment, J. Phys. Chem. C 120 (42) (2016) 24088–24097. doi:10.1021/acs.jpcc.6b06845.

[42] S. Tsuzuki, N. Kuzuu, H. Horikoshi, K. Saito, K. Yamamoto, M. Tani, Influence of oh-group concentration on optical properties of silica glass in terahertz frequency region, Applied Physics Express 8 (2015) 072402. doi:10.7567/apex.8.072402.

[43] B. Born, M. Havenith, Terahertz dance of proteins and sugars with water, Journal of Infrared, Millimeter, and Terahertz Waves 30 (12) (2009) 1245–1254. doi:10.1007/s10762-009-9514-6.
URL https://doi.org/10.1007/s10762-009-9514-6

[44] A. I. McIntosh, B. Yang, S. M. Goldup, M. Watkinson, R. S. Donnan, Terahertz spectroscopy: a powerful new tool for the chemical sciences?, Chem. Soc. Rev. 41 (2012) 2072–2082. doi:10.1039/C1CS15277G.
URL http://dx.doi.org/10.1039/C1CS15277G

[45] D. Sopu, J. Kotakoski, K. Albe, Finite-size effects in the phonon density of states of nanostructured germanium: A comparative study of nanoparticles, nanocrystals, nanoglasses, and bulk phases, Phys Rev B 83 (24). doi:10.1103/PhysRevB.83.245416.